

Recombination of Atoms at Surfaces

An Effusion Method Applied to Oxygen Atom Recombination

J. W. MAY* AND J. W. LINNETT†

From the Inorganic Chemistry Laboratory, Oxford University, Oxford, England

Received August 23, 1966; revised December 14, 1966

Recombination of O atoms on evaporated films of Ag, Cu, Au, and Cr was studied by an effusion method. Recombination efficiencies derived from measurements of heat liberated at the surface are in substantial agreement with other methods. The chance γ that an O atom colliding with the surface leaves as part of an O₂ molecule was measured for Ag and Cu films in the temperature range 300-375°K. For silver, $\gamma_{Ag} = 0.75 \exp(-720/RT)$ and for copper, $\gamma_{Cu} = 0.9 \exp(-1600/RT)$. For gold γ_{Au} was 6×10^{-3} at 305°K and 12×10^{-3} at 347°K. Chromium films gave erratic results. Films of Ag reacted with O atoms to produce AgO, and those of copper and chromium showed evidence of oxidation also. Films of Au were not tarnished by atomic O.

I. INTRODUCTION

This paper presents an effusion method for measuring the absolute efficiency of the recombination of atoms at surfaces. The efficiency γ is defined as the chance that an atom colliding with the catalytic surface leaves it as part of a diatomic molecule.

Nakada and co-workers (1, 2) have used "effusion" to establish an activity series for the recombination of hydrogen atoms on metals. A disc containing an interior thermocouple was coated on either side by a different metal. Presentation of each face to a jet of partially dissociated gas issuing from an orifice (not proper effusion) allowed an activity series to be established by comparing the temperature rises of two metals at a time. Other and different experiments in flow systems (3-7) have measured the change required in electrical power input to keep isothermal a metal filament exposed to atoms, and the recombination efficiency was calculated using the assumed atomic flux, the geo-

metrical area of the filament, and an independent measure of the atom concentration.

In the present experiments partially dissociated oxygen gas was allowed to effuse under the Knudsen conditions (8) into a vessel evacuated by a fast pumping system (Fig. 1). A fraction of the atoms struck a thin circular Pyrex detector disc coated with the active surface. The detector was mounted perpendicular to, and coaxial with, the effusion axis. Of those atoms that struck the disc face, a fraction γ would recombine there. The recombination efficiency was obtained from the electrical power corresponding to the heat of the atom association by knowing the atom to surface collision number determined by the effusion characteristics. The power developed by recombination was measured by a platinum resistance thermometer on the reverse side of the detector from the atom flux. Its resistance, which also measured the disc temperature, was an arm in a Wheatstone bridge circuit.

The power developed by the atom recombination was of the order 10^{-4} W, compared with about 1 W for typical flow system experiments. This disadvantage was

* Department of Engineering Physics, Cornell University Ithaca, New York.

† Professor of Physical Chemistry, University of Cambridge, Cambridge, England.

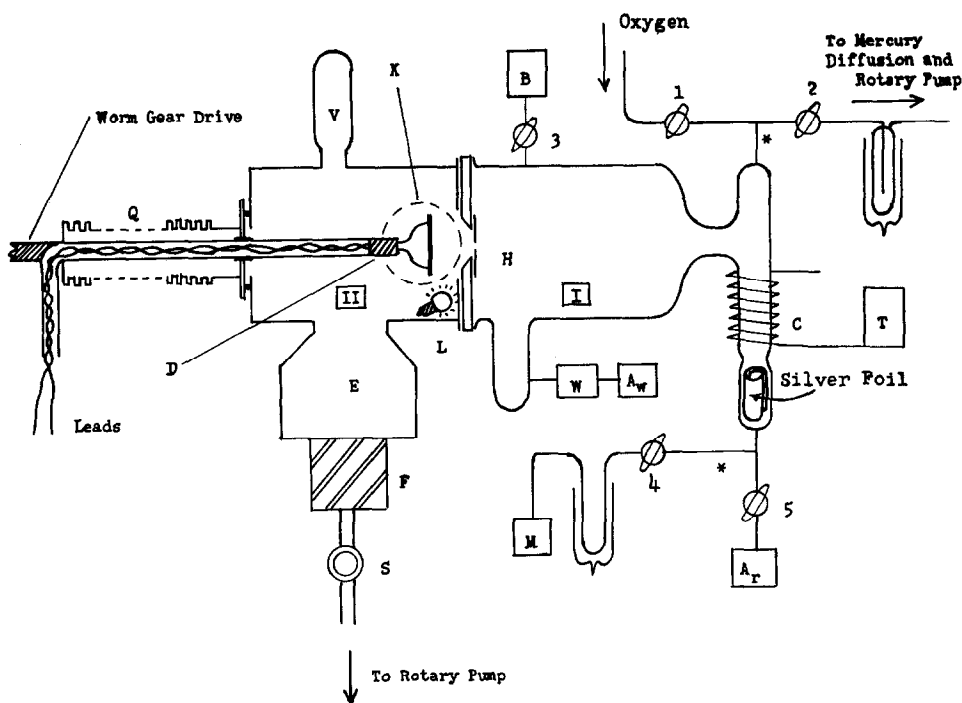


FIG. 1. Apparatus: O atoms were produced in a quartz tube by an electrodeless discharge at region of coil C (powered by rf transmitter T). Atoms diffused into Chamber I which had glass walls, and where total pressure was 10^{-2} torr, and eventually effused through orifice H into Chamber II (10^{-4} torr), which had brass walls. Atoms striking detector disc D (see Fig. 4) could liberate energy to disc by recombining into O_2 molecules at the catalytic film on the disc surface. Chamber II was pumped by fast oil diffusion pump F through cold trap E. The detector disc could be observed with illumination L through window K, and its distance from H adjusted by bellows drive Q. M is a McLeod gauge, and W a Wrede gauge for measuring O atom concentration. A_r , A_w , and B are micro-pirani (hot-wire) pressure gauges. Ionization gauge V measured pressure in Chamber II. Asterisks indicate positioning of Ag foil to prevent passage of O atoms, but there was no exposed metal between C and H. The large volume-to-surface ratio of Chamber II kept atom loss by recombination small. Chamber I was painted black to stop room light from reaching detector.

compensated for by a good knowledge of the atom flux, its angular distribution, and the geometry of the system. The sidearm diffusion method of Smith (9) which has been used extensively (10-18) gives γ as directly proportional to the atom/molecule diffusion coefficient (19-23). An advantage of the present method is its independence of the diffusion coefficient; measurements of γ by the Smith method, or modifications of it (24, 25), are only as accurate as that quantity. Moreover if the temperature variation of γ is investigated by a diffusion method, resort must usually be made to a semiempirical or theoretical estimation of the diffusion coefficient and its temperature

dependence. Another advantage of the new method is that it is best for very active surfaces of $\gamma > 10^{-2}$, which is just the region where methods based on diffusion become intractable (12, 26, 27).

True effusion into a vacuum through an orifice occurs when, as in these experiments, the mean free path on the high-pressure side is much larger than the orifice dimensions. If the effusant at P dynes/cm² is a partially dissociated gas having atom mole fraction α and the orifice is considered to have infinitesimally thin walls, then the number of atoms passing per second through the hole of area A is, according (28) to the kinetic theory,

$$A\alpha P[2\pi mkT]^{-1/2} \quad (1)$$

where m is the mass of the atom and k is Boltzmann's constant. In real systems the flow is less than predicted by (1) due to reflections from the orifice walls. Clausing (29) has calculated the reduced flow as a function of the diameter d and length l of the orifice considered as a cylindrical channel. The calculations also show that the angular distribution of the effusant is altered by the finite channel length. Compared with perfect effusion, the probability that the effusing molecules emerge at a large angle θ to the effusion axis is reduced. The effect calculated by Clausing may be expressed as

$$f = \int_0^{\theta_m} T(\theta, l, d) \sin 2\theta \, d\theta \quad (2)$$

In (2) f is the chance that a molecule of the effusant, after entering the channel of a real orifice, emerges on the other side within a cone whose sides are an angle θ_m to the effusion axis. $T(\theta, l, d)$ is a complicated function which reduces to 1 for perfect effusion when $f = \sin^2 \theta_m$. Equation (2) may be written in terms of a function B so that

$$f = B \sin^2 \theta_m \quad (3)$$

The orifice used in this work is shown in Fig. 2. The area measured by microprojection was $1.98 \times 10^{-3} \text{ cm}^2$ (mean diameter 0.050 cm). The length of the channel was 0.012 cm. B was calculated by numerical integration and the effect of the channel length for this work is shown in Fig. 3.

Although the orifice was not a point source of atoms the effect on the angular distribution was negligible. A formula derived by Keene (30) was applied and the maximum error in f was calculated as 0.1% from this effect.

The measurement of γ then depended on the following assumptions:

(i) That atoms which missed the detector never returned as atoms and also that those striking the detector face did so once only before being recombined on the brass walls of Chamber II or pumped (Fig. 1). Calculations based on the experimental

conditions show these assumptions to be justified because γ for the walls was almost certainly larger than 10^{-2} . The calculation also applied to the back of the detector which was protected by a resistant inactive varnish.

(ii) That atoms travel in straight lines to the detector from the orifice. This is justified by the background pressure.

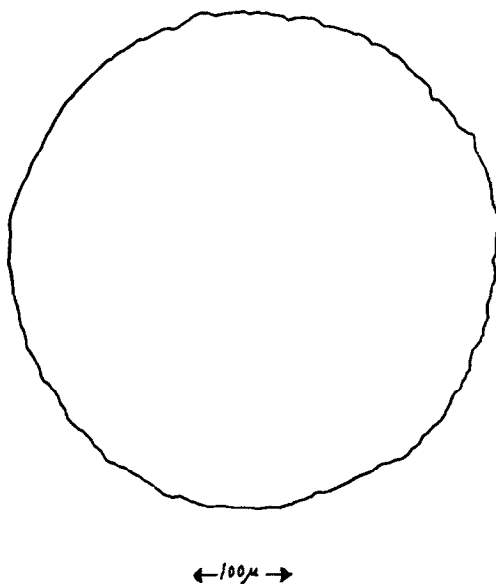


FIG. 2. Orifice cross section. The orifice was a hole drilled ultrasonically through 0.012-cm thick Pyrex disc; the disc was then cemented by shellac-based wax over a bevelled 1-cm hole centered in a Pyrex plate 2.5 mm thick. The bevel was 60° to the effusion axis (Fig. 1). $130\times$.

(iii) That the atom concentration at the detector is the same as the concentration measured on the high-pressure side by a Wrede-Harteck gauge.

(iv) That only ground state atoms (10) arrive at the detector.

(v) That there is negligible recombination within the short channel of the glass orifice. This is justified because γ for glass is very small, and the chance of atoms hitting the orifice walls is also small.

(vi) That the difference between the effusant temperature and that of the detector results in no measurable power loss. No cooling of the detector by accommodation was observed (detector temperature held between 30° and 100°C and pressure

of oxygen in chamber I varied sixfold with discharge off).

(vii) That electronically or vibrationally excited molecules do not release heat to the detector (see later).

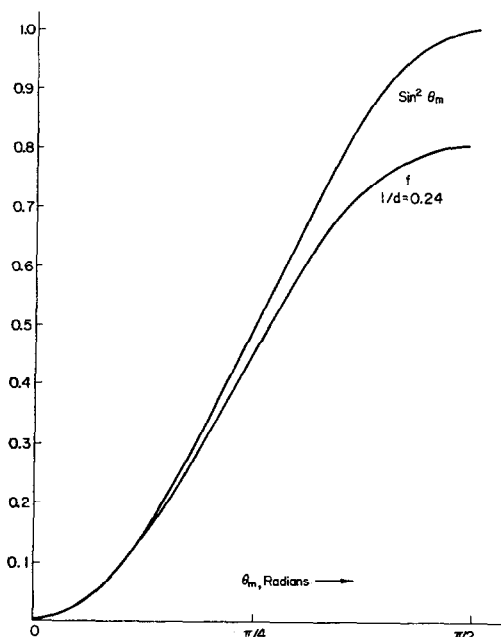


FIG. 3. Effect on angular distribution in effusion caused by dimensions of orifice. Lower curve is for the orifice used for this work [Eq. (3)].

(viii) That only electronic ground state molecules result from recombinations, and the whole dissociation energy is liberated to the surface (see later).

If D is the ground state dissociation energy in kcal/mole and N is Avogadro's number, the heat liberated per atom striking the detector is $0.5 \gamma D/N$. Using Eq. (1) the power H in watts developed by the recombination is, under the assumptions given,

$$H = 500JA\alpha fP(D/N)\gamma(2\pi mkT)^{-1/2}$$

or

$$\gamma = \frac{(8.194 \times 10^{-4})H(MT)^{1/2}}{A\alpha fDP_{mm}} = KH \quad (4)$$

where M is the atomic weight; J , joules/calorie, and P_{mm} , Chamber I pressure in

torr. In the present experiments, with $T = 300^\circ\text{K}$, and with oxygen atoms,

$$K = 0.243/\alpha fP_{mm} \quad \text{W}^{-1} \quad (5)$$

II. EXPERIMENTAL

1. Materials and Methods

a. Oxygen supply. Oxygen was obtained by electrolysis and leaked into the apparatus through a thermostated needle valve. The pressure behind the leak was kept at 740 torr automatically. During experiments oxygen flowed towards the orifice H in competition with the very much larger flow maintained by the pumping line (Fig. 1). With this arrangement a stable pressure could be maintained in Chamber I, and fresh oxygen would continually pass into the silica discharge tube.

b. Positioning of detector disc. The detector could be moved towards or away from the orifice in vacuum, and was held by a detachable steel bellows system. A steel tube, lined up with the effusion axis, carried the leads away from, and ultimately supported, the detector. The tube was connected to a worm gear drive, allowing relative positions of the detector to be read to 0.02 mm in a movement of 37 mm. The platinum wire (40 swg) leads from the detector were set in a jack-plug connection to the supporting tube. The bellows system, seated on an O-ring, could be unscrewed and the detector passed out through a 1-inch hole. During experiments Chamber II (Fig. 1) was maintained at 25°C to prevent random temperature fluctuations in the region surrounding the detector.

c. Measurement of the atom concentration by Wrede-Harteck gauge. A differential micro-Pirani Wheatstone bridge was used, similar to that of Greaves and Linnett (13). A micro-Pirani hot wire gauge of a design similar to theirs, A_w (Fig. 1), was connected to the Wrede-Harteck gauge, W . During an experiment the equilibrium pressure difference ΔP that developed between the interiors of A_w and a reference micro-Pirani A_r was measured as an effective change in resistance across the bridge, in which the hot tungsten wires of A_w and

A_r were opposite resistances. It may be shown that

$$\alpha = 3.41(\Delta P)/P$$

To calibrate the bridge A so that ΔP and hence α could be calculated, another bridge B was used. With the valve S and taps 1 and 2 closed (Fig. 1), taps 3, 4, and 5 open, the micro-Pirani B could be first calibrated against the McLeod gauge M. Then with tap 4 closed and an imposed pressure difference between Chamber I and the interior of the McLeod gauge, the differential bridge A was calibrated. During experiments with atoms the reference micro-Pirani A_r was separated from the discharge plasma by a section of 4-cm Pyrex tubing containing a cylindrical lining of silver foil 10 cm long. The effect was to prevent atoms reaching A_r without permitting a pressure difference to develop. During experiments tap 3 was closed. The micro-Pirani gauges, which had no temperature-compensating leads, were thermostated by water flowing through brass cases which enclosed them almost completely. The Wrede gauge W had a volume of about 15 cc, and the calculated 99% equilibration time (1β) was 5 sec. The Wrede gauge consisted of a B24 cone ground flat to accommodate a circular cover slip containing a central hole of 0.05-mm diameter. After the interior had been lined with silver foil, the cover slip was cemented into position with Araldite resin.

d. Detector-disc heating elements. Resistance thermometer elements were prepared with Liquid Bright Platinum 05-X (Hanovia). The method was due to Vidal (31). Pyrex discs, 2-cm diameter and 0.012 cm thick, were washed in chloroform, then painted with a zigzag line passing across the disc so that each bend was near the circumference. After the discs had been fired they were immediately removed from the oven and allowed to cool rapidly in the laboratory air. Platinum leads were soldered to the shiny film using the flux recommended by Vidal. After testing the soldered joints for strength, each detector was water-washed, dried, and the circuit side only painted over with Atlas Epidura var-

nish. The varnish both protected the circuit and strengthened the disc. Evaporated metal films, after use, could then be removed by acid and the disc used anew. Detector discs are shown in Fig. 4.



FIG. 4. Detector disc. Mounted on jack plug, and unmounted, showing platinum resistance thermometer (wavy line on back of disc).

e. Atom heat detection bridge. The resistance of the detector element, R_a , was balanced against a resistance box R (0–1111 ohms) in a standard Wheatstone bridge. The other two fixed arms determined the bridge ratio of 24.93. The emf across the bridge was provided by two 6-V accumulators in series. The potential across the bridge was adjusted by two other resistances, a fine and a coarse one, respectively in series and parallel with the supply. The potential across R_a could be measured by two potentiometers I and II connected in series and using a potential divider of 1.270 and 3 K, so that the true emf across R_a was divided by 3.36. Out-of-balance current was observed on a galvanometer G, which was shunted by 470 ohms and was in series with a variable sensitivity control 0–10 K.

f. Detector discs as resistance thermometers. The temperature coefficient of resistance of each detector heating element was obtained using the atom heat detector bridge with the detector placed in a furnace heated to 200°C. The resistance of the detector was measured as the furnace was allowed to cool, and temperature near the

detector was measured at the same time by a thermojunction. Linear variation of resistance with temperature was obtained, and for the 12 heating elements used in this work the mean temperature coefficient of resistance was $1.86 \pm 0.18 \times 10^{-3}$ per $^{\circ}\text{C}$, in good agreement with Vidal (31). The fired paint had a resistance of about 3 ohms/square. Variability in resistance was caused by nonreproducibility of paint thickness. Most of the resistance thermometers had resistances between 100 and 150 ohms.

g. Production of the discharge; screening and pickup. Radiofrequency power was generated from the oscillator and output stages of an RCA transmitter type ET-4336-H at 13.75 Mc/sec (32). The discharge was produced within a copper coil. In most cases 100 W of rf power were dissipated. The coil was "tank" tuned so as to antiphase nodal radiation from the ends. The oxygen discharge was usually an intense flamingo pink at 10^{-2} torr, and was checked from spreading by earthed copper chokes. All circuitry was carefully screened, as had been found mandatory by Greaves and Linnett (13). Bridges and galvanometer movements were housed in earthed metal containers. Brass housings around the micro-Pirani gauges screened the filaments inside. However, electrical pickup on the sensitive bridges was a recurring and persistent cause of trouble, probably due to a semisaturated earth connection to the screening. Pickup was reduced to a tolerable level by adjusting the earth connections with the aid of an oscilloscope. To check that the atom detector bridge had the necessarily negligible deflection due to pickup, conditions of a recombination experiment were simulated except that the face of the detector was left as clean glass. The recombination heat liberated on such a face should be unobservable in our experiments (γ of the order 10^{-4}). Pickup was therefore considered absent only when essentially no deflection was observed away from balance of the atom detector bridge when a reasonable atom concentration was indicated by the Wrede gauge bridge. Frequent checks were re-

quired and were made. Pickup and its possible effect on the measurement of atom concentration caused the greatest uncertainty in the results.

h. Destruction of atoms by activation of Chamber I. No atoms were recorded at the detector after long times of operation. It was inferred that part of the interior of Chamber I became catalytically active for a reason not discovered. This gradual process did not affect calculation of γ as both H and α of Eq. (4) decreased in proportion. If the glassware from the discharge tube to the orifice was dismantled it could be deactivated by soaking in dilute nitric acid, but unfortunately deactivation did not last for more than about 15 discharge hours, after which another dismantling would be needed.

i. Preparation of evaporated metal films. Evaporated metal films were prepared by standard technique (33, 34) in a 10-inch bell jar under a background pressure less than 10^{-5} torr. Films were prepared from Johnson and Matthey Specpure silver, gold, and chromium. Copper films were made from CP pellets. The copper and gold (as foil) were lightly pickled in decinormal nitric acid and washed in distilled water before use. Silver, copper, and gold were evaporated from molybdenum boats, chromium and copper from tungsten baskets. Copper films from either source appeared the same. During evaporation, the source was covered by a hemispherical Pyrex mask with a 1-inch hole just above the source. Each detector to be coated was supported upside down by its leads so that its face was about $\frac{3}{4}$ inch above the mask exit. The impurity concentration of the films was estimated from the data of Heavens (35) to be less than 1 part in 10^4 . In the case of chromium there was some doubt about purity because the source was often slightly etched after evaporation. All films were estimated to have thickness in the range 0.3–1.5 μ , and had high reflectivity and the appearance of the bulk metal. That the films be as little contaminated as possible, they were only exposed to the air for a few minutes, the time necessary to remove them from the evaporation unit and

mount them inside Chamber II, which was then at once evacuated.

2. Measurement of the Electrical Power Equivalent of Recombination

When the discharge is turned off, the detector disc cools. Its resistance thermometer changes resistance by ΔR_d and there is a change of potential across it ΔV . If the resistance with the discharge on is R_d ohms and the potential drop across it V and if V_{exptl} is the experimental value measured by the two potentiometers I and II connected in series as has been described (see Section II,e), then

$$V/3.36 = V_{\text{exptl}} = V_I + V_{II} \quad (6)$$

$$1/R_d = 24.93/R - 1/(1270 + 3000) \quad (7)$$

The electrical power equivalent H of recombination can then be written

$$H = \Delta(V^2/R) = 2V\Delta V/R_d - (V/R_d)^2\Delta R_d \quad (8)$$

Two methods were used to measure H which we call the Isothermal and the Cooling Curve Methods. In the Isothermal Method the discharge was turned off and the change in voltage across R_d required to return R_d to its value with the discharge on was measured. In the Cooling Curve Method, an analysis was made based on the detector's cooling curve when the discharge was turned off. This cooling curve was related to the time change of the out-of-balance current developed across the detector bridge after the discharge had been turned off. In (8), $\Delta V = V_o - V_a$ and $\Delta R_d = (R_d)_o - (R_d)_a$. The presence, or not, of atoms at the detector is indicated by the subscripts *a* and *o*.

a. Isothermal method. Using (6), (7), and (8) and the condition that ΔR_d is made zero for this method (see above) and assuming the other resistances in the bridge to be unaltered,

$$H_i = (3.36)^2(2V_{\text{exptl}}\Delta V_{\text{exptl}})[(24.93/R) - 1/4270] = (3.36)^2U \quad (9)$$

where U is the power difference in watts actually measured and ΔV_{exptl} is the change ΔV_{II} , V_I being held constant.

b. Cooling curve method. Consider the atom heat bridge at balance. If R were altered $+1$ ohm, the galvanometer spot of G would move a distance ΔG . The spot should be returned to the null position by changing R_d by $+1/24.93$ ohms, because both the bridge current and V would not be appreciably changed (R_d was of the order 100 ohms in most cases). It was possible to obtain for each detector element, when Chamber II was held at the experimental pressure of 2×10^{-6} torr, a calibration curve $\Delta R/\Delta G$ as a function C of R ,

$$(dR/dG)_R = C \quad (10)$$

Also it was found empirically that under the same conditions a graph of V_{exptl} versus R gave a good straight line for each detector. That is

$$\Delta V_{\text{exptl}} = b\Delta R \quad (11)$$

Using (6), (7), (8), (10), and (11), and neglecting the term $1/4270$ of (7), one obtains

$$H_c = (3.36)^2(24.93)V_{\text{exptl}}(\Delta G/R)C[2b - (V_{\text{exptl}}/R)] = (3.36)^2W \quad (12)$$

Measurements of both H_i and H_c could be made for each experiment, by first taking the cooling curve after the discharge was stopped and then readjusting R by rebalancing the bridge. In some of the experiments, especially when the detector was coated with copper, gold, or chromium, H_c alone was measured without setting the galvanometer exactly at the null position before turning off the discharge. Any resultant error in ΔG was negligible. The value of ΔG was measured from each cooling curve by an extrapolation of the final section of the curve to the moment when the discharge was turned off. This was necessary because the detector temperature was often slowly changing due to a very gradual fluctuation of the ambient radiation flux. The isothermal measurements, because of drifting background temperature, could easily give values of ΔV_{exptl} with large errors. Values of b for the detectors were usually close to 2.5×10^{-3}

ohm/V, and values of C were usually between 0.1 and 0.8 ohm/cm of galvanometer scale.

Measurements of recombination efficiency by the isothermal method are denoted γ_i and by the cooling curve method γ_c . It is useful to use a quantity Z obtained from (5), (9), and (12)

$$Z = \frac{1}{(3.36)^2 K} = \frac{U}{\gamma_i} = \frac{W}{\gamma_c} = \frac{H_i}{(3.36)^2 \gamma_i} = \frac{H_c}{(3.36)^2 \gamma_c} \quad (13)$$

c. Details of an experiment. After the detector with its metal film had been mounted inside Chamber II, the distance-measuring counter was brought to zero when the detector was coplanar* with the interior face of Chamber II. Using the counter the detector was then set at a known distance from the orifice, and the amount of the effusant that would hit the detector face could be calculated by (3). The pumps were turned on and 3 or 4 hr were allowed for the apparatus to come to equilibrium. When the experiment was to begin, the temperature of the detector was set and the discharge was struck after the Wrede gauge bridge and the atom detector bridge had both been approximately balanced. After allowing at least 15 min for equilibration, the pressure at the McLeod gauge was read and the balance point of the Wrede bridge A recorded (Section II,c). The galvanometer spot for the atom detector bridge was then brought near the null position from the side corresponding to excess detector heat by adjusting the fine voltage control supplying this bridge. With the greater part of V_{expt1} backed off by potentiometer I, the remainder, which was about 0.1% of V_{expt1} , was read with potentiometer II. Potentiometer I was constantly restandardized so that a small drift in the emf of its batteries was not magnified as a large error in the reading of potentiometer II. The two voltages V_I and V_{II} were then recorded, and a power Variac controlling the discharge turned to zero.

* This was possible owing to the bevel described in captions to Figs. 1 and 2.

The spot of galvanometer G then moved to the direction corresponding to a cooling of the detector, and its position was recorded at 30-sec intervals until the detector was clearly again at thermal equilibrium. The equilibration time was usually about 5 min. The spot G was then brought back to the null position and V_{II} again recorded. Bridge A was then out of balance because the pressures in the Wrede gauge and the reference Pirani had again become equal (Section II,1,c). Bridge A was rebalanced and the differential resistance corresponding to a known atom concentration was recorded. The pressure was then again measured by the McLeod gauge. All the data were then available for calculating γ by Eq. (5).

III. RESULTS

1. Preliminary Experiments

Early attempts to measure atom recombination heats were nonreproducible because of heating by room light. The heating effect of the light could be as much as ten times that to be expected from atom recombination on silver. Light was therefore excluded by painting chamber I black.

Figure 5 shows typical behavior for turning the atom discharge first on, then off. Deflections were observed for the galvanometers of both the Wrede and atom bridges, as well as for the pressure measured with the McLeod gauge. For this experiment the detector was coated with silver. The slow overall change in the temperature of the detector shows the effect of a changing ambient radiation. A pressure drop, fairly reproducible on a given day, was nearly always observed on striking the discharge. The effect was usually smaller than shown in the figure, but tended to increase as the pressure in Chamber I was lowered. The pressure drop may be explained in the following way: On striking the discharge a momentary rise in pressure would be expected from dissociation of molecules, but the former equilibrium pressure would be reattained were it not for the fact that the number flow through the orifice is increased for a partially disso-

ciated gas. A net lowering of the pressure by this mechanism would be enhanced by the higher efficiency of the mercury diffusion pump, which was previously operating near its upper limit. But total pressure read at the McLeod gauge was assumed to be the same as in the discharge tube and in Chamber I during an experiment. (The

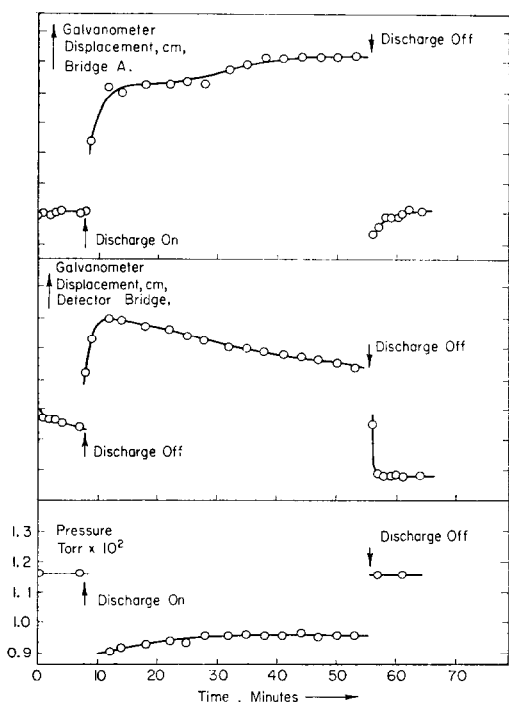


FIG. 5. Effect of turning discharge on and off. Typical displacements of galvanometers of the atom-concentration and detector-heating bridges, and a simultaneous change in pressure recorded at the McLeod gauge. Displacement of Bridge A resulted from atoms diffusing from discharge into Chamber I. The detector bridge measured heat produced by atom recombination at probe D (Figs. 1 and 4).

calculated linear flow of gas towards the orifice was only 0.5 cm/sec at 10^{-2} torr.) Pressure drops such as that of Fig. 5 necessitated a correction to the apparent atom concentration because bridge A was balanced both during an experiment and after the discharge was turned off, when the pressure reverted to its original value. The correction was obtained from the small change in bridge balance for which a calibration

had previously been determined. It was usually less than 1 part in 20.

Typical cooling curves for the evaluation of γ_c are given in Fig. 6. The figure shows the loss in sensitivity for a silver catalyst when a detector of high resistance was used. On the other hand, the detector

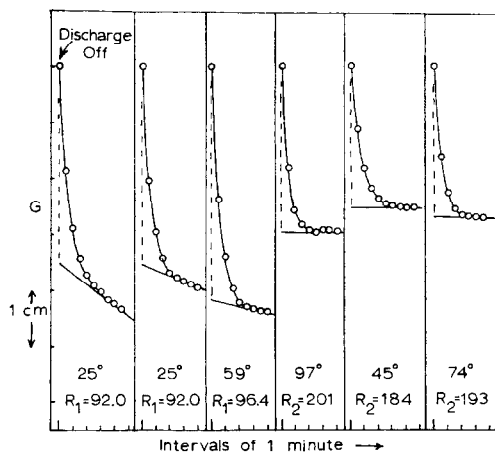


FIG. 6. Cooling curves for silver catalyst after discharge turned off. Displacement of galvanometer extrapolated at zero time in each case proportional to heating power of recombining atoms. Results for two different resistance thermometers R_1 and R_2 are shown. (Resistances in ohms, temperatures in $^{\circ}\text{C}$.)

with higher resistance produced a larger ΔV_{exptl} for equivalent activity, therefore more accurate values of γ_1 . The slopes of the extrapolated lines indicate the drift in the detector due to ambient radiation changes. When the slope was large, so was the discrepancy between γ_1 and γ_c .

2. Proportionality between Recombination Heat and Atom Concentration

Experiments to test direct proportionality between recombination heat and atom concentration according to Eq. (4) were performed on silver. The detector-to-orifice distance as well as the resistance R were kept constant throughout. Combining Eqs. (4) and (12) permits definition of a quantity Y proportional to γ which should have been constant during the experiments assuming that γ did not change with time. This is shown in Table 1.

TABLE 1
PROPORTIONALITY OF RECOMBINATION HEAT TO A QUANTITY Y FOR A SILVER-COATED DETECTOR^a

Arbitrary units of power dissipated in the discharge	Mole fraction of atoms α	P (torr) $\times 10^2$	Galvanometer displacement ΔG (cm)	Y (cm/torr) $\times 10^{-2}$
80	0.32	1.15	2.69	7.3
100	0.41	1.10	3.45	7.6
120	0.49	1.13	4.00	7.2
120	0.52	1.11	4.30	7.4
120	0.48	1.14	3.85	7.0
130	0.57	1.16	4.40	6.7
130	0.54	1.11	4.07	6.8

^a $Y = \Delta G/P\alpha$, at constant detector temperature and position.

3. Relation between Atom Recombination Heat and Detector-to-Orifice Distance

Another set of experiments was carried out to determine whether the atom recombination heat varied with detector-to-orifice distance in the manner predicted by the theory of effusion. The detector was again coated with silver. The recombination heat was measured isothermally. The results according to Eq. (13) are shown in Fig. 7(a). The detector-to-orifice distance was varied between 0.93 and 2.03 cm, corresponding to extreme values of θ_m of about 48° and 24°. It was not possible to alter the detector-to-orifice distance and then simply remeasure γ , because the amount of background radiation falling on the detector changed as well when the detector was moved. Thus every point of Fig. 7(a) represents an individual experiment under equilibrium conditions. The good straight line of the figure has a slope of 0.80 ($= \gamma_1$). It was observed after the experiment upon removal of the film that the film had begun to peel, because the experiments were made before the evaporation technique had been perfected. There was also evidence of a bluish-white deposit which may have been an oxidized impurity originally introduced into the film during its deposition. That γ for silver in this case was about treble the activity shown by all other silver films was attributed either to the increased surface area or to the impurity. Peeling of the film was not observed subsequent to these experiments.

Two other sets of experiments were performed varying the detector-to-orifice dis-

tance, again with silver as the catalyst. In one case the heat was measured isothermally, and in the other by the cooling curve method. These results are shown in Fig. 7(b). That the lines did not pass through the origin is attributable to a small amount of electrical pickup. In any case the results clearly demonstrate the soundness of the assumptions with respect to effusion.

4. Recombination of O Atoms on Silver

Over half the experiments in the present investigation were done on silver. Disc temperatures were varied between room temperature and 100°C, and total pressure in Chamber I was in the range $0.65 \times 10^{-2} < P < 1.37 \times 10^{-2}$ torr. The lowest measured mole percent of atoms was 29%, the highest 58%. Most of the experiments were done with the plane of the detector 1.30 cm from the orifice; other distances used were between 0.73 cm and 2.08 cm. In all the experiments there was visual evidence of oxidation. Discs coated with silver, after exposure to O atoms, always showed several concentric sets of brilliantly colored iridescent rings centered on the effusion axis. Colors such as red, yellow, green, and blue gave a rainbow effect, presumably due to a thin oxide layer.

The recombination efficiency was calculated by both the isothermal and cooling curve methods. Both gave similar results. In 45 of the 84 experiments on silver, values of both γ_1 and γ_0 were obtained. That there was no significant bias is clear because the average difference $\frac{1}{45}\sum\gamma_1 - \gamma_0$ was only 0.025 for these cases. A least-

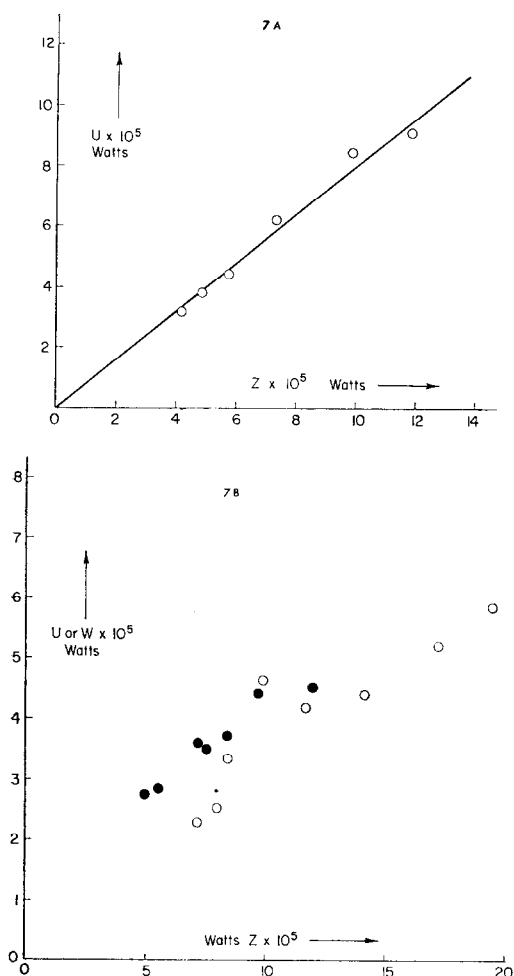


Fig. 7. Effect of changing detector-to-orifice distance. The graph shows the proportionality between recombination heat and atom arrival rate when the latter is altered by changing the detector-to-orifice distance. Effusant temperature assumed to be 300°K . Graphs plotted according to Eq. (13). (a) Preliminary experiment on contaminated film; slope = $\gamma_1 = 0.80$, detector at 91°C . (b) Comparison of isothermal and cooling curve methods for two different detector discs (different resistances). Filled circles, isothermal method (U) with detector at 53°C ; open circles, cooling curve method (W) with detector at 94°C .

squares treatment of all 84 of the experimental values as an Arrhenius plot gave the equation for $298^\circ < T < 375^\circ\text{K}$,

$$\gamma(\text{silver}) = (0.75 \pm 0.35) \exp - [(720 \pm 350)/RT]$$

Values of γ from experiment to experiment showed considerable scatter, as indicated by the uncertainties just given. This scatter was presumably due to differences between films, such as adsorbed impurities, sintering effects, or uncertainties in the atom concentration. If, however, a set of experiments was carried out for the same film, and without changing the atom concentration, the temperature effect and its size could be clearly demonstrated. Results for three such sets of experiments are given in Fig. 8. The Arrhenius lines drawn

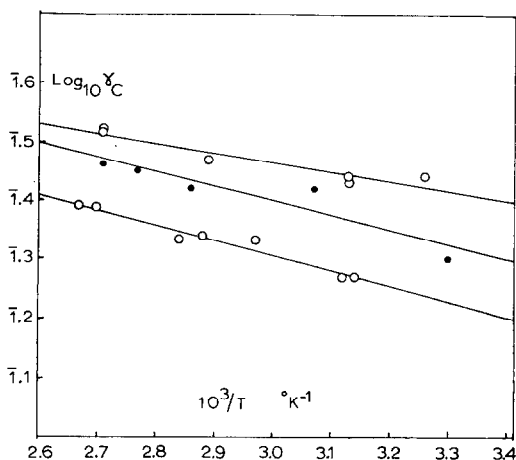


Fig. 8. Arrhenius lines for recombination of O atoms on silver. Figure shows data for three sets of experiments on three different films. Activation energies are (top to bottom) 740, 1140, and 1180 cal/mole.

through each of these sets corresponded to activation energies of 740, 1140, and 1180 cal/mole (top, middle, and lowest curve in that order), or an average of 1020 cal/mole for the three lines.

It was sometimes noted that on a new silver film values of γ in a set of measurements tended to increase a little with total time of exposure. The differences were small and not always observed. Myerson (36) has reported the same effect for O atoms on silver. He observed that silver reached its maximum activity after a very short exposure to atoms. Strutt (37) has also commented on this effect.

5. Recombination of O atoms on Copper

Experiments on copper were again confined to a small pressure range, $8.35 \times 10^{-3} < P < 1.19 \times 10^{-2}$ torr. The temperature range was between room temperature and 100°C . The concentration of atoms varied between 21% and 59% of total gas. Only γ_c was measured and it appeared to be more variable on copper than on silver films. This may be due to the smaller recombination heat on copper being more

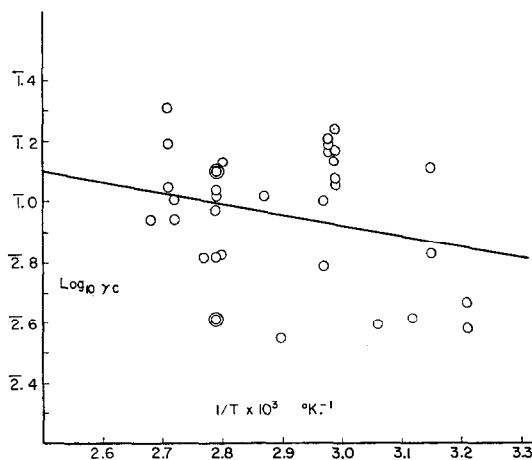


FIG. 9. Arrhenius line for recombination of O atoms on copper. All experimental points that were obtained are plotted. Figure shows the degree of scatter inherent in these experiments. Activation energy of least-squares line (shown) is 1600 cal/mole.

difficult to measure. As for silver, every copper film exposed to the atom flux showed evidence of oxidation. The metal became discolored by a thin golden-brown coating, and on one occasion, with the largest atom concentrations, a multicolored oxide film was produced, brownish yellow in the center passing through blue to red at the perimeter. All the values obtained for γ_c on copper are shown in the Arrhenius plot of Fig. 9. A least-squares treatment of the points gave the equation

$$\gamma(\text{copper}) = (0.9 \pm 2.4) \exp \left[- \frac{(1600 \pm 1100)}{RT} \right]$$

The central values in the equation give a value for γ (copper) at 300°K of 6.3×10^{-2} , a factor of 3 smaller than silver. The

experiments on copper included several checks that the recombination heat decreased with increasing detector-to-orifice distance, but there was considerable scatter.

6. Experiments on Gold and Chromium

Only four measurements were made of γ (gold). The results were uncertain because the efficiency was so small. A detector of low resistance (about 33 ohms) was used to increase the sensitivity so that γ_c could be measured. The average of two values for γ_c at 32°C was 6.1×10^{-3} , and of two values at 74°C was 1.2×10^{-2} , equivalent to an activation energy of 3 ± 2 kcal/mole. These values should be taken as upper limits of γ . There was no evidence of oxidation of the film.

The results for chromium were unfortunately widely spread because the pressures were low, $7.8 \times 10^{-3} < P < 1.06 \times 10^{-2}$ torr. Also, lower atom concentrations than in the other experiments were recorded, between 17% and 25% of total gas. The situation was aggravated by the low activity of the films. Fifteen measurements were made altogether, between 35° and 83°C . The values of γ_c were so scattered that we only report the mean value of all the experiments of $\gamma(\text{chromium}) = 6 \pm 4 \times 10^{-2}$. One set of experiments showed a temperature coefficient corresponding to about 1 kcal/mole, though in general the results showed too much scatter to be certain of a temperature effect. Some of the chromium films did not show oxidation, but one did after long exposure to atoms. The oxide film was an iridescent sky-blue color, and developed after over 7 hr of continuous operation.

With the assumption that the recombination efficiency can be expressed

$$\gamma = \gamma_\infty \exp(-E/RT) \quad (14)$$

the results of the present work are summarized in Table 2.

7. Bulk Oxide formed by O Atoms at a Silver Surface

It has been observed that silver, in the presence of O atoms, is eventually oxidized

TABLE 2
 SUMMARY OF THE RESULTS

Metal	Temperature range (°C)	Variation of γ over temperature range	γ_{∞}	E (kcal/mole)
Silver	25-102°	0.22-0.29	0.75 ± .35	0.72 ± .35
Copper	39-100°	0.070-0.11	0.9 ± 2.4	1.6 ± 1.1
Gold	32-74°	0.0061-0.012	~2	3 ± 2
Chromium	35-83°	Mean = 0.06	—	(~1)

to a black bulk oxide (10, 12, 36, 37). Linnett and Marsden (10) showed that introduction of some of it into a manganese solution produced the purple coloration of the permanganate ion, showing that it was a powerful oxidant. The exact nature of the oxide had not been determined. We have investigated some of its properties.

The reaction of oxygen atoms from the discharge with silver foil under two sets of conditions led to two different oxide coatings. With the pressure less than 2×10^{-2} torr and the foil placed outside but near the plasma and exposed about 8 hr, the foil became covered with a loosely held layer of shiny black oxide. The yield was about 1.5 mg/sq. cm at an atom concentration of 80% or more. In the early stages of oxidation the foil exhibited multicolored patterns of oxide over the whole spectrum of colors, in a fashion similar to those observed at the detector disc after O atoms had been recombined on a silver film. In an effort to increase the yield the foil was placed inside the plasma and the pressure raised to 5×10^{-2} torr. In this case the oxide was formed in two layers, a thin black layer on top of a thick dark brown sublayer. The yield did not increase significantly.

The black oxide showed oxidizing power.

Any touching the fingers released a strong smell of ozone. A few mg in a mixture of 10 ml of 3M KI solution, 2 drops of conc. H_2SO_4 , and 2 ml of CCl_4 produced a purple color in the CCl_4 after 10-fold dilution and addition of dilute silver nitrate to destroy triiodide.

Two separately prepared samples of the fresh black oxide (A and B) and one 6-week-old sample (C) were chemically analyzed, as well as a sample of the brown oxide (D). A modified method of analysis due to Palmer was used (38). The weighed oxide was reduced with standard oxalic acid and the excess determined with standard $KMnO_4$ solution. Total silver was obtained by a Volhard titration (Table 3).

The brown-black oxide might be written $AgO \cdot Ag_2O$. Somewhat low assays for silver(II) or its equivalent may be expected using this method of analysis (39). The fresh oxide was evidently AgO . The old sample (C) showed evidence of some decomposition, but the analysis was doubtful because the sample was very small.

Two other tests were made of the black oxide. X-Ray powder diffraction photographs were taken from two separate freshly prepared samples. The reflections agreed very well with the monoclinic spacings that have been assigned to AgO (40-42). We are most grateful to Mr. K. Wat-

 TABLE 3
 ANALYSIS OF OXIDE FORMED AT THE SILVER SURFACE

Sample	Actual weight (g)	Calculated weight (g)	Calculated wt. of silver (g)	Calculated wt. of oxygen (g)	Calculated formula
A	0.0179	0.0176	0.0155	0.0021	$Ag_{1.09}O$
B	0.0178	0.0177	0.0156	0.0021	$Ag_{1.10}O$
C	—	0.0076	0.0069	0.0007	$Ag_{1.6}O$
D	0.0412	0.0418	0.0383	0.0035	$Ag_{1.64}O$

son for obtaining the photographs. In addition to the X-ray data, the magnetic susceptibility was measured by Mr. J. P. Day on a Faraday balance as $+0.37 \times 10^{-6}$ emu/g, in fair agreement with Klemm (43) but not with other authors (41, 44, 45).

At sufficiently low pressures, then, and when bulk oxide is formed, we conclude that it is AgO. At higher pressures a mixture of AgO and Ag₂O is very likely produced.

IV. DISCUSSION

The present experiments demonstrate that an effusion technique is feasible and that it also offers an independent check of methods based upon diffusion. This can be seen from Table 4, where we have com-

TABLE 4
RECOMBINATION OF O ATOMS AT
ROOM TEMPERATURE

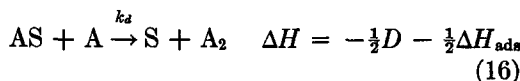
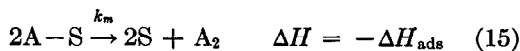
Metal or Oxide surface	γ	Reference
Ag	0.24	12
	0.15	23
	0.22	This paper
Cu	0.17	12
	0.15	23
	0.063	This paper
Cu ₂ O	0.11	16
CuO	0.043	12
	0.020	13
	0.045	16
Cr	~ 0.06	This paper
Cr ₂ O ₃	0.00025	13
Au	0.0052	12
	0.0061	This paper

pared the present results with previous data for Ag, Cu, Au, Cr, and their oxides. The effusion results compare favorably with the others in the table.

Because O atoms attack metals so readily, the study of their recombination at an unoxidized metal surface is probably impossible in most cases. After exposure to O atoms, most clean metals will rapidly become covered with an oxide layer which

may or may not have the same catalytic activity as the virgin surface. In the case of silver there is evidence that the oxide is more active than the metal (36, 37), but for copper and chromium the reverse seems to be the case. There are other examples of such effects. For instance, Linnett and Marsden (11) found that activities of Pd and Pt foils for recombining O atoms decreased with time, and Fryberg and Petrus (46) attributed variability of Pt for O atom recombination to surface oxidation.

Two main mechanisms are available for atom recombination. They are (i) the recombination of two adatoms represented by Eq. (15), or (ii) the combination of an adatom with one striking it from the gas phase, represented by Eq. (16). These are known as (i) the Langmuir-Hinshelwood mechanism (LH) and (ii) the Bonhoeffer-Farkas-Rideal mechanism (BFR).



ΔH_{ads} refers to the differential heat of adsorption of the diatomic molecule at the equilibrium coverage during recombination. It is negative if the adsorption process is exothermic, which chemisorption of O₂ has always been observed to be. D is the heat of dissociation of the diatomic molecule; it is positive. The rate constants of (15) and (16) are k_m and k_d . Because for O₂ ΔH_{ads} is ordinarily negative and D is positive, (16) may be either exothermic or endothermic depending on the coverage and the metal. At very high coverages, ΔH_{ads} usually becomes small, and therefore ΔH of (16) might approach the limiting value of $-D/2$, hence it is very probable that this process is always exothermic between intermediate and high values of the coverage. For oxygen, however, Eq. (15) will usually be strongly endothermic and should only be possible at high temperatures.

A complete kinetic treatment to permit decision on which of (15) or (16) is theoretically rate-controlling has been given by Ehrlich (47) and extended by Dickens,

Linnett, and Palczewska (18). The conclusion is that near room temperature and at pressures not too low, the BFR mechanism (16) dominates, and the kinetics will be unambiguously first order in O atoms. (In fact, at temperatures close to room temperature, first order kinetics have always been observed for recombination of either H or O atoms.) The reasonable assumptions on which Ehrlich (47) based his treatment are (a) atoms have unit sticking probability on unoccupied sites (this may not be quite the case but it should provide a fair approximation), (b) molecules have much lower sticking probability, (c) the rate of evaporation of atoms as atoms is negligible. It may then be shown, if E_a is the activation energy corresponding to k_d , that

$$\gamma_{\text{BFR}} = \frac{2k_d}{1+k_d} \quad 0 < k_d < 1 \quad (17)$$

$$\theta_{\text{BFR}} = \frac{1}{1+k_d} = 1 - \frac{\gamma}{2} \quad (18)$$

$$\frac{d \ln \gamma_{\text{BFR}}}{d(1/T)} = \frac{-E_d}{R} \left(1 - \frac{\gamma}{2}\right) = \frac{-\theta E_d}{R} \quad (19)$$

According to (18) the coverage θ of catalytically active sites lies between the limits 0.5 and unity, depending on whether

γ is large or small. For this range of coverage we have already concluded that (16) is most probably always exothermic, so that one is tempted to apply Hirschfelder's Rule (48), which predicts an upper limit for E_a of $0.055 D = 6.5$ kcal/mole for O atom recombination. Our present results are in agreement with this prediction, as are all other published data for recombination of O atoms on metal surfaces. Application of (19) using our room temperature values of γ and the experimental activation energies at 300°K, gives $E_a = 0.8$ kcal/mole for silver and 1.7 kcal/mole for copper.

It is interesting to compare energies for processes occurring at the surface during atom recombination. This is done in Fig. 10. In the figure ΔH_{atom} represents the bond energy with the surface of adsorbed atoms, and other symbols have the same meanings as before. Three cases are considered. (a) ΔH_{ads} is exothermic and $\Delta H_{\text{atom}} < D$; (b) ΔH_{ads} is exothermic and $\Delta H_{\text{atom}} > D$; (c) ΔH_{ads} is endothermic and $\Delta H_{\text{atom}} < \frac{1}{2} D$. The first of these (a) applies to silver and copper, the second (b) to tungsten (49) and possibly to chromium, and the third (c) applies to gold. The diagram shows that for case (a) ΔH of reaction (16) is always less exothermic than $\frac{1}{2} D$, but for

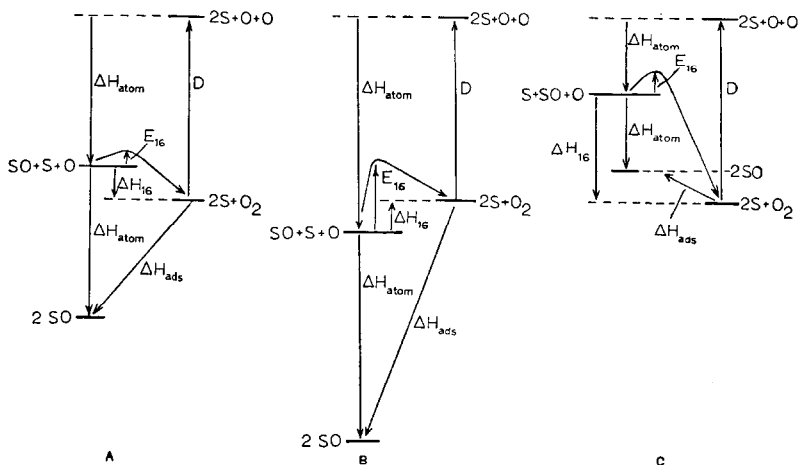


Fig. 10. Energetics of O atom recombination according to Eq. (16). D is the dissociation energy of O_2 , S represents a surface site, ΔH_{atom} is the atom-to-surface bond energy, ΔH_{ads} is the heat of adsorption of O_2 , E_a and ΔH_{16} are the activation energy and the heat of reaction of Eq. (16). (A) $\Delta H_{\text{atom}} < D/2$ and ΔH_{ads} is exothermic. (B) $\Delta H_{\text{atom}} > D/2$ and ΔH_{ads} is exothermic. (C) $\Delta H_{\text{atom}} < D/2$ and ΔH_{ads} is endothermic.

case (c) (16) is *more* exothermic than $\frac{1}{2}D$. For case (b) reaction (16) is predicted to be endothermic by an amount less than $\frac{1}{2}D$, or in other words, recombination of O atoms in a *primary* adsorbed layer will not be expected to proceed spontaneously, although recombination via a second adlayer, adsorbed above a strongly held primary layer, cannot be ruled out. In that event, however, the situation would be formally analogous to case (a).

The foregoing analysis can be applied when we consider how much energy is liberated in the rate-controlling step (16). Wood, Mills, and Wise (7) have reported that H₂ molecules, formed by the catalyzed recombination of H atoms on surfaces of Ni, W, or Pt, leave the surface with excess vibrational energy so that energy transfer to the surface is incomplete. They report that as little as 0.2 of the dissociation energy of H₂ is transferred to the solid during recombination. In view of the fact that recombination of atoms by the BFR mechanism is a *two-step process*, and that chemisorption of H₂ on all three of these metals is exothermic, case (a) of Fig. 10 must be operating. In other words, theory predicts a minimum of $0.5D$ of heat liberated at the surface for each recombined molecule formed, and a maximum of $0.5D$ that might escape in the newly formed molecule as excess kinetic or internal energy. It seems to us likely that only a small fraction of this maximum energy could be carried away in the case of O atom recombination, and that for H atom recombination the results of Wood, Mills, and Wise (7) are extremely difficult to understand. Further support for this comes from the experiments of Larkin and Thrush (50), who concluded that after atom recombination, molecules of O₂, H₂, or N₂ leave surfaces of Ag, Cu, Ni, or Pt with an average of not more than twice the thermal velocity corresponding to the surface temperature.

This last result is of considerable importance for the present method. If some excess energy is carried away by O₂ molecules formed according to reaction (16), values of γ obtained in this work might conceivably be too low, but not by more

than a factor of 2. We believe thermal accommodation at the surface of newly formed O₂ molecules to be essentially complete.

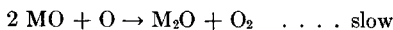
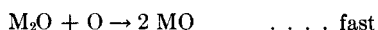
It has been claimed by Reeves, Mannella, and Harteck (51) that combination of atoms at surfaces can lead to the formation of electronically excited molecules. This was not observed by them for O atoms *alone*, but was for N atom recombination, and also when both N and O atoms were present. In the latter case excited NO was observed. In our view it is very unlikely that in the present experiments electronically excited O₂ molecules could leave the strong perturbation field of the surface, because only ground state ³P O atoms are present in the type of discharge used by us (10, 11, 19, 52).

We have so far concluded that the heat of association measured in these experiments has not been appreciably decreased by the carrying away of excess kinetic energy nor by the formation of electronically excited O₂ molecules. We must still consider the possibility of extra heat being released to the surface by vibrationally excited or electronically excited molecules from the discharge. Such molecules would, on average, make a great number of collisions with the walls of Chamber I (Fig. 1) before reaching the detector face. It seems reasonable to assume that by the time such molecules reached the catalyst surface they would have become de-excited if such transitions were not forbidden. If they are forbidden, it seems unlikely that appreciable deexcitation should then occur on the catalyst surface. We must, however, point out evidence for the existence of such excited molecules (53-56). Foner and Hudson (55) and Elias, Ogryzlo, and Schiff (56) inferred the presence, in the products of an oxygen discharge, of the long lived ¹Δ_g state, which is 22.6 kcal/mole above the ground state. The latter authors, using a calorimetric probe in a flow system, showed that considerable heat was liberated at the probe after the discharge products had been first passed over a mirror of mercury, which removed all O atoms from the stream. Yet, because of the excel-

lent agreement of the present results with other methods which are independent of heat transfer to the surface and on the basis of the agreement presented at the beginning of this paragraph, we believe that excited molecules did not significantly affect the present results.

One last source of extra heat remains. Not all the atoms arriving at the surface are combined into O₂ molecules. Some are incorporated into the metal surface as oxide, releasing heat in the process, but the chance of this happening is small. For example, the observed rate of formation of AgO was 0.2 mg/cm² per hr at 10⁻² torr and 80% atomic gas. From this the chance of an O atom being permanently held as AgO after arrival at a silver surface can be calculated as about 6 × 10⁻⁵. In other words, it is about 4000 times more probable that an O atom is recombined to give O₂ than that it is incorporated to form AgO at room temperature.

We conclude this discussion with the comment that a possible BFR mechanism on either silver or copper might be conceived as proceeding in a thin oxide film possessing higher and lower oxidation states (11, 13, 36). If both divalent and monovalent metal ions are in the surface, the mechanism might be expressed by the following equations:



This is a more complex picture than was put forward earlier in this discussion, but may well be an important feature of O atom recombination on transition metal surfaces.

ACKNOWLEDGMENTS

One of us (J.W.M.) thanks the British Oxygen Company for a maintenance Fellowship. We are indebted to the British Oxygen Company and to the U.S. Air Force for supplying some of the equipment.

REFERENCES

1. NAKADA, K., SATO, S., AND SHIDA, S., *J. Chem. Soc. Japan* **76**, 1308, 1313 (1955).
2. NAKADA, K., *Bull. Chem. Soc. Japan* **32**, 809, 1072 (1959).
3. ROGINSKII, S. Z., AND SHEKTER, A. B., *Acta Physiochim. URSS* **1**, 318 (1934); *ibid.* **6**, 401 (1937).
4. BUBEN, N., AND SHEKTER, A. B., *Acta Physiochim. URSS* **10**, 371 (1939).
5. FOX, J. W., SMITH, A. C. H., AND SMITH, E. J., *J. Chem. Phys.* **31**, 265 (1959); *Proc. Phys. Soc.* **73**, 533 (1959).
6. FRANTCHEVITCH, I. N., AND LAVRENKO, V. A., *Dokl. Akad. Nauk SSSR* **148**, 1137 (1963).
7. WOOD, B. J., MILLS, J., AND WISE, H., *J. Phys. Chem.* **67**, 1462 (1963).
8. KNUDSEN, M., "Kinetic Theory of Gases," 3rd ed. Methuen, London, 1950.
9. SMITH, W. V., *J. Chem. Phys.* **11**, 110 (1943).
10. LINNETT, J. W., AND MARSDEN, D. G. H., *Symp. Combust., 5th, Pittsburgh, 1954*, p. 685 (1955).
11. LINNETT, J. W., AND MARSDEN, D. G. H., *Proc. Roy. Soc. (London)* **234A**, 489, 504 (1956).
12. GREAVES, J. C., AND LINNETT, J. W., *Trans. Faraday Soc.* **54**, 1323 (1958).
13. GREAVES, J. C., AND LINNETT, J. W., *Trans. Faraday Soc.* **55**, 1346, 1355 (1959).
14. GREEN, M., JENNINGS, K. R., LINNETT, J. W., AND SCHOFIELD, D., *Trans. Faraday Soc.* **55**, 2152 (1959).
15. PROK, G. M., *Chem. Abstr.* **55**, 18253 (1961); *ibid.* **56**, 2915 (1962).
16. DICKENS, P. G., AND SUTCLIFFE, M., *Trans. Faraday Soc.* **60**, 1272 (1964).
17. DICKENS, P. G., AND WHITTINGHAM, M. S., *Trans. Faraday Soc.* **61**, 1226 (1965).
18. DICKENS, P. G., LINNETT, J. W., AND PALCZEWSKA, W., *J. Catalysis* **4**, 140 (1965).
19. KRONGELB, S., AND STRANDBERG, M. W. P., *J. Chem. Phys.* **31**, 1196 (1959).
20. WALKER, R. E., *J. Chem. Phys.* **34**, 2196 (1961).
21. WEISSMAN, S., AND MASON, E. A., *J. Chem. Phys.* **36**, 794 (1962).
22. YOUNG, R. A., *J. Chem. Phys.* **34**, 1292 (1961).
23. HARTUNIAN, R. A., THOMPSON, W. P., AND SAFRON, S., *J. Chem. Phys.* **43**, 4003 (1965).
24. WOOD, B. J., AND WISE, H., *J. Chem. Phys.* **29**, 1416 (1958); *J. Phys. Chem.* **65**, 1976 (1961); *ibid.* **66**, 1049 (1962).
25. WISE, H., AND ROSSER, W. A., *Symp. Combust., 9th, 1962*.
26. WISE, H., AND ABLOW, J., *J. Chem. Phys.* **29**, 634 (1958).
27. DICKENS, P. G., SCHOFIELD, D., AND WALSH, J., *Trans. Faraday Soc.* **56**, 225 (1959).
28. KENNARD, E. H., "Kinetic Theory of Gases." McGraw-Hill, New York, 1938.

29. CLAUSING, P., *Z. Physik* **66**, 471 (1930); *Ann. Phys.* **7**, 489 (1930); *ibid.* **12**, 961 (1932).
30. KEENE, H. B., *Proc. Roy. Soc. (London)* **88A**, 49 (1913).
31. VIDAL, R. J., Cornell Aeronaut. Lab. Report WADC TN56-315 (1956).
32. GREAVES, J. C., JENNINGS, K. R., AND LINNETT, J. W., U.S. Air Force Report AF61(514)-1117 (1959).
33. HOLLAND, L., "Vacuum Deposition of Films." Chapman and Hall, London, 1958.
34. PIRANI, M., AND YARWOOD, J., "Principles of Vacuum Engineering." Chapman and Hall, London, 1961.
35. HEAVENS, O. S., *Proc. Phys. Soc. (London)* **65B**, 788 (1952).
36. MYERSON, A. L., *J. Chem. Phys.* **38**, 2043 (1963).
37. STRUTT, R. J., *Proc. Phys. Soc. (London)* **23**, 66 (1910).
38. PALMER, W. G., "Experimental Inorganic Chemistry." Cambridge Univ. Press, Cambridge, England, 1954.
39. McMILLAN, J. A., *Chem. Rev.* **62**, 65 (1962).
40. McMILLAN, J. A., *J. Inorg. Nucl. Chem.* **13**, 28 (1960); *Acta Cryst.* **7**, 640 (1954).
41. SCATTURIN, V., BELLON, P., AND SALKIND, A. J., *J. Electrochem. Soc.* **108**, 819 (1961); SCATTURIN, V., BELLON, P., AND ZANNETTI, R., *J. Inorg. Nucl. Chem.* **8**, 462 (1958).
42. GRAFF, W. S., AND STADELMAIER, H. H., *J. Electrochem. Soc.* **105**, 446 (1958).
43. KLEMM, W., *Z. Anorg. Chem.* **201**, 32 (1931).
44. NEIDING, A. B., AND KAZARNOVSKII, I. A., *Dokl. Akad. Nauk SSSR* **78**, 713 (1951).
45. SELBIN, J., AND USATEGUI, M., *J. Inorg. Nucl. Chem.* **20**, 91 (1961).
46. FRYBERG, G. C., AND PETRUS, H. M., *J. Chem. Phys.* **32**, 622 (1960).
47. EHRlich, G., *J. Chem. Phys.* **31**, 1111 (1959).
48. HIRSCHFELDER, J. O., *J. Chem. Phys.* **9**, 645 (1941).
49. BRENNAN, D., HAYWARD, D. O., AND TRAPNELL, B. M. W., *Proc. Roy. Soc. (London)* **A256**, 81 (1960).
50. LARKIN, F. S., AND THRUSH, B. A., *Nature* **197**, 375 (1963).
51. REEVES, R. R., MANNELLA, G. G., AND HARTECK, P., *J. Chem. Phys.* **32**, 946 (1960); *ibid.* **33**, 636 (1960).
52. RAWSON, E. B., AND BERINGER, R., *Phys. Rev.* **88**, 677 (1952).
53. BROIDA, H. P., AND GAYDON, A. G., *Proc. Roy. Soc. (London)* **A222**, 181 (1954).
54. BRANSCOMB, L. M., *Phys. Rev.* **86**, 258 (1952).
55. FONER, S. N., AND HUDSON, R. L., *J. Chem. Phys.* **25**, 601 (1956).
56. ELIAS, L., OGRYZLO, E. A., AND SCHIFF, H. I., *Can. J. Chem.* **37**, 1680 (1959).